Carbonyl Sulfide: Potential Agent of Atmospheric Sulfur Corrosion

Abstract. *Laboratory exposure experiments demonstrate that carbonyl sulfide in wet air corrodes copper at 22°C at a rate that is approximately linear with total exposure (the product of exposure time and carbonyl sulfide concentration). The corrosion rate is similar to that of hydrogen sulfide, a widely recognized corrodant. The much greater average atmospheric abundance of carbonyl sulfide compared with that of hydrogen sulfide or sulfur dioxide suggests that carbonyl sulfide may be a major agent of atmospheric sulfur corrosion.*

Corrosion of materials results in large economic costs to society. Estimates of the magnitude of these costs in the United States alone range from $4.1 billion (*1*) to $70 billion (*2*) annually. A large but difficult to quantify fraction of these costs results from sulfur corrosion, which is generally thought to be due to airborne sulfur dioxide (SO_2) (*1*) and, to a lesser extent, hydrogen sulfide (H_2S) (*3*). Sulfur corrosion is readily attributable to nearby emission sources such as coal combustion furnaces (SO_2) or marshes (H_2S), but it also occurs in areas well removed from such sources. (Perhaps the most easily recognized example of the latter is the ubiquitous tarnishing of silverware.) Some perspective on the relative concentration of atmospheric sulfur-containing molecules is provided in Table 1, in which data from urban and industrial areas are compared with those from remote locations. It is immediately apparent that H_2S and SO_2 dominate the spectrum of urban sulfur-containing gases, at least near strong sources. In contrast, carbonyl sulfide (OCS) has a near uniform concentration throughout the global troposphere and is the most abundant sulfur-containing molecule in nonurban areas. Integration over the entire atmosphere indicates that OCS is the predominant global sulfur-bearing compound (*4*).

Little is known of the corrosivity of OCS, particularly under ambient conditions. Experience with pressurized cylinders containing OCS demonstrates that the gas is noncorrosive at 25°C when dry but decomposes relatively rapidly in the presence of water, with the resulting corrosion of susceptible materials (*5*). This decomposition is expressed stoichiometrically as (*6*)

$$OCS + H_2O \rightarrow H_2S + CO_2$$

although the chemical system is almost certainly more complex, potentially involving a number of intermediates. Since H_2S is known to be corrosive, especially at high humidities (*7–9*), the hypothesis that OCS is an atmospheric corrosive agent in humid air is a reasonable one. Accordingly, we have carried out experiments in which we have exposed copper to OCS in carefully controlled humid atmospheres and determined the resulting sulfidation. This report describes the results of these experiments.

We prepared the copper samples by electroplating oxygen-free, high-conductivity copper onto scanning electron microscope (SEM) specimen mounts made from the same material and then subjecting them to a sequential mechanical polish (*10*). The result is a surface with a roughness estimated from SEM studies to be 0.6 μm. The samples were rinsed first in ethanol and then in distilled water to "degrease" the surfaces and were exposed to OCS in the experimental arrangement described in (*9*), except that

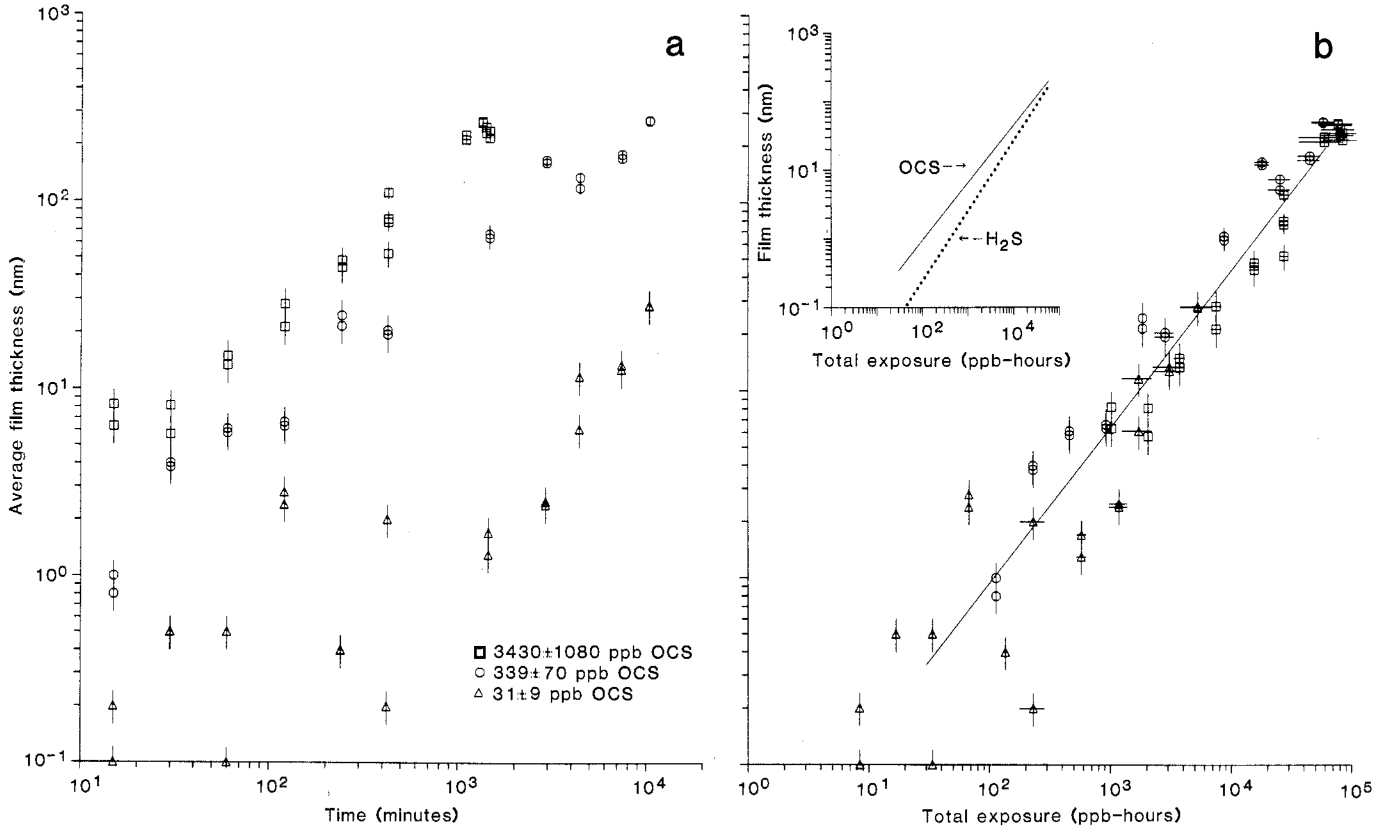

Fig. 1. (a) Sulfide film thickness as a function of exposure time for different OCS concentrations. All exposures were made within the experimental ranges temperature = 20° ± 2°C and relative humidity = 80 ± 4 percent. (b) Sulfide film thickness as a function of total exposure to OCS. The solid line is a least-squares fit to the data points. The inset compares the rate of copper corrosion by OCS to that produced by H_2S exposure, as determined under the same experimental conditions (*9*).

0036-8075/81/0508-0663$00.50/0 Copyright © 1981 AAAS

Table 1. Concentrations of atmospheric sulfur gases; ppt, parts per trillion.

Species	Urban and industrial areas		Remote areas	
	Concentration (ppt)	Reference	Concentration (ppt)	Reference
H_2S	15 to 5000	(*24*)	5 to 50	(*25*)
CS_2	70 to 370	(*26, 27*)	25 to 45	(*27*)
CH_3SCH_3	No data		42 to 62	(*28*)
OCS	430 to 570	(*29*)	430 to 570	(*29*)
SO_2	10^3 to 10^6	(*24*)	50 to 120	(*30*)

the gas supply is a mixture of 11 parts per million (ppm) OCS in N_2, diluted appropriately and with O_2 added to make a preselected concentration of OCS in 21 percent O_2 and 79 percent N_2. [The H_2S contamination in commercial OCS mixtures is typically < 0.2 percent of the OCS concentration (*5*) and is therefore of concern in these experiments only if the observed corrosion rates are so low that they might be attributable to an impurity of that order of magnitude.] We varied the water content of the air by adjusting the portion of the air supply that passes through a humidifier. A dew-point hygrometer and hot-wire anemometer were used to monitor the dew point and flow rate continuously. One determines the OCS concentration by converting the OCS to SO_2 over an oxidizing catalyst and measuring the resultant SO_2 by pulsed resonance fluorescence (*11*). An important feature of the system is the provision for continuous analysis of the OCS concentration, which eliminates the potential for undetected concentration reductions resulting from OCS loss to wet chamber walls or other surfaces. Each sensor is sampled once per minute throughout the exposure period; the resulting values for the exposure conditions are derived from statistical analyses of these data by a dedicated desk-top computer system.

We studied the thickness and morphology of the copper sulfide films with an SEM (Kent-Cambridge Stereoscan 2A) equipped with a solid-state x-ray detector and a multichannel analyzer. The thicknesses of the corrosion films were determined by energy-dispersive x-ray analysis (EDXA). The preparation of thickness standards necessary for this method, described in (*12*), consists of the vapor deposition of copper films onto silicon substrates, measurement of their thicknesses by microscopic viewing of cleaved cross sections, and exposure to H_2S *in wet air to fully* sulfidize the copper. The sulfidized films are then floated off the silicon and remounted onto bulk copper substrates to obtain thickness standards of copper sulfide on copper. The ratios of the sulfur and copper x-ray intensities for these standards (as measured by EDXA) thus constitute a calibration curve of film thickness as a function of the intensity ratio. If sulfur concentration gradients in the bulk copper are disregarded and the sulfur is assumed to be present as Cu_2S (*8, 9*), the average film thicknesses can be determined with an estimated accuracy of 20 percent or ±8 nm, whichever is smaller.

The results of our experiments (Fig. 1a) show that OCS readily forms sulfide films on copper. The rate of film formation appears to be a monotonic function of the OCS concentration. To explore this characteristic in more detail, we computed for each sample the total exposure, which is the product of the length of exposure of that sample and the average OCS concentration during that exposure (Fig. 1b). Within the accuracy of our data, the formation of sulfide film by OCS in humid ambient atmospheres appears to be a linear function of total exposure. The inset in Fig. 1b compares the corrosion rate of OCS to that produced by H_2S under similar temperature and humidity conditions. The rates are essentially equivalent, particularly for film thicknesses ≥ 5 nm, where our determinations become increasingly more accurate.

Qualitative support for our inference that OCS may be important in sulfide corrosion is provided by the limited literature on the subject. Iron undergoes sulfidation at 300° to 900°C in atmospheres containing OCS (*13, 14*), and OCS decomposition in the adsorbed phase is inferred to be among the mechanisms involved (*14*). Copper and silver corrosive film growth is better correlated with the reduced sulfur content of the atmosphere than with other pollutant parameters (*15*). Rice *et al.* assumed the reduced sulfur to be present as H_2S, S_8, or CH_3SH. We have followed their analytical procedure (*16*) with filters exposed to OCS, however, and find that OCS gives a positive response. Hence at least a portion of the correlation between silver and copper corrosive film growth and airborne reduced sulfur may be attributable to atmospheric OCS.

The average atmospheric concentration of OCS appears to be reasonably well determined and to be relatively uniform throughout the troposphere (implying a long lifetime). The magnitudes of the sources and sinks of OCS are less well known. This gas is generated by microbial activity (*17*), volcanoes (*18*), natural and agricultural fires (*19*), and a variety of industrial processes (*20*); although the natural sources appear to dominate, the few flux estimates that have been made are clearly preliminary. The principal loss mechanisms for OCS are diffusion to the stratosphere (*21*) and perhaps hydrolysis in the oceans (*22*). Because of the broad geographical scale of most of these processes, we expect the corrosive effects of OCS to be much more widespread than those of corrodants with spatially concentrated sources and short atmospheric lifetimes.

In summary, we have established that OCS corrodes copper at a rate essentially comparable to that of corrosion by H_2S. The much greater atmospheric abundance of OCS suggests that it may be a major agent of atmospheric sulfur corrosion (*23*).

T. E. GRAEDEL
G. W. KAMMLOTT
J. P. FRANEY

Bell Laboratories,
Murray Hill, New Jersey 07974

References and Notes

1. L. B. Barrett and T. E. Waddell, *Cost of Air Pollution: A Status Report* (Report AP-85, Environmental Protection Agency, Research Triangle Park, N.C., 1973).
2. L. H. Bennett, J. Kruger, R. L. Parker, E. Passaglia, C. Reimann, A. W. Ruff, H. Laskowitz, E. B. Berman, *Economic Effects of Metallic Corrosion in the United States* (Special Publication 511-1, National Bureau of Standards, Washington, D.C., 1978).
3. H. C. Wohlers and M. Feldstein, *J. Air Pollut. Control Assoc.* **16**, 19 (1966); J. Gerhard and F. H. Haynie, *Air Pollution Effects on Catastrophic Failure of Metals* (Report EPA-650/3-74-009, Environmental Protection Agency, Research Triangle Park, N.C., 1974).
4. R. P. Turco, R. C. Whitten, O. B. Toon, J. B. Pollack, P. Hamill, *Nature (London)* **283**, 283 (1980).
5. W. Braker and A. L. Mossman, *Matheson Gas Data Book* (Matheson Gas Products, East Rutherford, N.J., ed. 5, 1971), p. 115.
6. G. Buchbock, *Z. Phys. Chem.* **23**, 123 (1897); H. W. Thompson, C. F. Kearton, S. A. Lamb, *J. Chem. Soc.* **1935**, 1033 (1935); R. J. Ferm, *Chem. Rev.* **57**, 621 (1957).
7. P. Backlund, B. Fjellstrom, S. Hammarback, B. Maijgren, *Ark. Kemi* **26**, 267 (1966).
8. S. P. Sharma, *J. Electrochem. Soc.* **127**, 21 (1980).
9. J. P. Franey, T. E. Graedel, G. W. Kammlott, in *Proceedings of International Symposium on Atmospheric Corrosion* (Electrochemical Society, Princeton, N.J., in press).
10. M. E. Davis and T. J. Louzon, *Metallography* **13**, 195 (1980).
11. W. J. Zolner, D. J. Mager, D. A. Helm, "Application Note: Source Level SO_2 Analysis via

Pulsed Fluorescence" (Thermo Electron Corporation, Waltham, Mass., March 1972).
12. G. W. Kammlott, *Appl. Spectrosc.*, in press.
13. A. Hayden and S. Streiten, *Oxid. Met.* **3**, 545 (1971); *ibid.* **7**, 46 (1973); A. Rahmel, *Corros. Sci.* **13**, 125 (1973).
14. P. Hadjisavas, M. Caillet, A. Galerie, J. Besson, *J. Electrochem. Soc.* **127**, 569 (1980).
15. D. W. Rice, R. J. Cappell, W. Kinsolving, J. J. Laskowski, *ibid.*, p. 891.
16. J. A. Lorenzen, *Adv. X-Ray Anal.* **18**, 568 (1975); D. Hobgood and J. A. Lorenzen, *Finnigan Spectra* **5** (No. 2), RTP 17 (1975); D. F. S. Natusch, J. R. Sewell, R. L. Tanner, *Anal. Chem.* **26**, 410 (1974).
17. D. F. Adams, S. O. Farwell, M. R. Pack, W. L. Bamesburger, *J. Air Pollut. Control Assoc.* **29**, 380 (1979).
18. R. D. Cadle, *Rev. Geophys. Space Phys.* **18**, 746 (1980).
19. P. J. Crutzen, L. E. Heidt, J. P. Krasnec, W. H. Pollack, W. Seiler, *Nature (London)* **282**, 253 (1979).
20. T. E. Graedel, *Chemical Compounds in the Atmosphere* (Academic Press, New York, 1978), p. 315.
21. P. J. Crutzen, *Geophys. Res. Lett.* **3**, 73 (1976).
22. F. S. Rowland, paper presented at the 4th international conference of the Commission on Atmospheric Chemistry and Global Pollution, Symposium on Budgets and Cycles of Trace Gases and Aerosols in the Atmosphere, Boulder, Colo., 1979.
23. Experiments to establish the dependence of the corrosion rate on temperature and humidity, to study the effects of OCS on other materials, and to derive mechanistic information are in progress.
24. T. E. Graedel, in *Handbook of Environmental Chemistry*, O. Hutzinger, Ed. (Springer, Heidelberg, 1980), vol. 2, part A, p. 107.
25. B. J. Slatt, D. F. S. Natusch, J. M. Prospero, D. L. Savoie, *Atmos. Environ.* **12**, 981 (1978); A. B. Goldberg, P. J. Maroulis, L. A. Wilner, A. R. Bandy, *ibid.*, in press.
26. F. J. Sandalls and S. A. Penkett, *ibid.* **11**, 197 (1977).
27. P. J. Maroulis and A. R. Bandy, *Geophys. Res. Lett.*, in press.
28. ———, *Science* **196**, 647 (1977).
29. P. J. Maroulis, A. L. Torres, A. R. Bandy, *Geophys. Res. Lett.* **4**, 510 (1977); A. L. Torres, P. J. Maroulis, A. B. Goldberg, A. R. Bandy, *J. Geophys. Res.*, in press.
30. P. J. Maroulis, A. L. Torres, A. B. Goldberg, A. R. Bandy, *ibid.*
31. We thank C. J. Weschler for valuable discussions.

6 October 1980; revised 27 January 1981

Miocene Stable Isotope Record: A Detailed Deep Pacific Ocean Study and Its Paleoclimatic Implications

Abstract. *Deep Sea Drilling Project site 289 in the western equatorial Pacific has yielded an extremely detailed record of the carbon and oxygen isotopic changes in the Miocene deep ocean. The isotopic record reflects major changes in paleoclimate and paleoceanography, probably dominated by a major phase of Antarctic ice-cap growth. The transition from a relatively unglaciated world to one similar to today occurred between 16.5 × 10⁶ and 13 × 10⁶ years before the present, with the greatest change occurring between approximately 14.8 × 10⁶ and 14.0 × 10⁶ years before the present.*

We present here a detailed record of the stable isotopes of oxygen and carbon of Miocene benthic foraminifera from equatorial Pacific Deep Sea Drilling Project (DSDP) site 289. The record depicts Miocene climatic changes and permits speculation on the causes of the major changes in the earth's climate that occurred during the Miocene epoch, 5.5×10^6 to 22×10^6 years before the present (B.P.).

The results of this study are indicative of an early Miocene world characterized by relatively limited polar glaciation and by deep ocean waters significantly warmer than the near freezing waters of today. By late Miocene time, a large Antarctic ice cap existed and ocean temperatures approached today's values. The data presented document a rapid transition to an extensively glaciated world in early middle Miocene time.

DSDP site 289 on the Ontong-Java Plateau (00°29.92′S, 158°36.69′E) was chosen for this study because its thick, continuously cored Miocene section contains abundant, well-preserved foraminifera. It is located near the plateau crest and hence is free from sources of downslope contamination. Its water depth (2200 m) has probably been maintained by its high sedimentation rate, 36 to 71 m per 10^6 years (*1*).

Oxygen and carbon isotopic compositions of well-preserved foraminifera reflect the isotopic compositions of, respectively, the H_2O and HCO_3^- in seawater, as well as the water temperature during test growth (*2*). Disequilibrium (biological) isotopic effects may also affect the isotopic composition of the tests. Almost all the 200 samples that we analyzed were monospecific samples of the benthic foraminiferal genus *Cibicidoides*. Comparison of $\delta^{18}O$ and $\delta^{13}C$ values of different species of *Cibicidoides* from single sediment samples indicated no significant interspecific differences in isotopic compositions. Hence the $\delta^{18}O$ values of different *Cibicidoides* species used in this study may be directly compared. However, all *Cibicidoides* species studied appear to be depleted in ^{18}O relative to calcite in isotopic equilibrium with seawater by about 0.65 ± 0.15 per mil (*3*). The $\delta^{13}C$ values of the Miocene benthic foraminifera analyzed probably change primarily in response to changes in the $^{13}C/^{12}C$ ratio of seawater HCO_3^-. In the analyses, we used standard techniques (*2*); results are reported in δ notation relative to the Pee Dee belemnite standard (PDB).

The age determinations were based on planktic foraminiferal biostratigraphy (*1*, *4*), and we correlated the ages to the geochronologic-biostratigraphic framework (*5*) by assuming a constant sedimentation rate between biostratigraphic marker horizons.

Isotopic results are plotted in Fig. 1a, with additional detail shown in Fig. 1b. Oxygen isotopic data indicate a general but irregular decrease in ^{18}O from approximately +1.5 per mil 20×10^6 years B.P. (planktic foraminiferal zone N5) to an average of about +1.0 per mil and a minimum of +0.66 per mil 16.3×10^6 years B.P. The lowest $\delta^{18}O$ value, 0.66 per mil, corresponds to the inferred warmest bottom water or minimum polar ice, or both, found in this study. From 16.3×10^6 to 14.8×10^6 years B.P. $\delta^{18}O$ values increased gradually to approximately +1.5 per mil, and at that time the character of the record changed markedly. The oscillations between 14.8×10^6 and 14.2×10^6 years B.P. in cores 45 and 47 (Fig. 1b) are striking. The difference between $\delta^{18}O$ values of adjacent samples (at approximately 6000-year intervals) has an average value of 0.22 per mil and a maximum of 0.58 per mil. A change in the benthic foraminiferal fauna at site 289 occurs in the same time range (*6*).

The remainder of the middle Miocene section and the lower part of the upper Miocene section (planktic foraminiferal zones N12 through N17) are characterized by $\delta^{18}O$ values that are uniformly higher than those of the early Miocene. The $\delta^{18}O$ values vary between approximately 2.0 and 2.8 per mil. The latest Miocene record (5×10^6 to 7×10^6 years B.P.) shows only minor $\delta^{18}O$ variation about a mean value of approximately 2.4 per mil.

Interpretation of paleotemperatures from the isotopic data requires knowledge of the $^{18}O/^{16}O$ ratio of seawater at the time the foraminifera grew. The isotopic record described above reflects a combination of temperature change and change in the volume and isotopic composition of continental ice. We have attempted to set limits on the Miocene bottom-water temperatures and isotopic compositions at site 289.

We assume that throughout Miocene time, as at present, bottom water formed as a result of the sinking of cold, dense surface water in Antarctic coastal regions, and hence that bottom-water temperatures were similar to coastal Antarc-